

# Thermal Conductivity of Mixtures of Carbon Dioxide and Ethane in the Critical Region

R. Mostert · J. V. Sengers

Received: 4 April 2008 / Accepted: 19 June 2008 / Published online: 24 July 2008  
© Springer Science+Business Media, LLC 2008

**Abstract** Experimental data are presented for the thermal conductivity of mixtures of carbon dioxide and ethane. The thermal conductivity has been measured with a parallel-plate instrument, as a function of temperature along isochores, so as to obtain detailed information on the behavior of the thermal conductivity of a mixture near the locus of vapor–liquid critical points. The experimental results are in agreement with theoretical predictions from the mode-coupling theory for critical dynamics in binary mixtures.

**Keywords** Carbon dioxide · Critical azeotropy · Critical region · Ethane · Thermal conductivity

## 1 Introduction

The thermal conductivity of one-component fluids is known to diverge at the critical point [1,2]. However, the behavior of the thermal conductivity of fluid mixtures near

---

R. Mostert  
Van der Waals-Zeeman Institute, University of Amsterdam, Valckenierstraat 67,  
1018 XE Amsterdam, The Netherlands

*Present Address:*

R. Mostert  
Corus Research Development & Technology, P.O. Box 10000, 1970 CA,  
IJmuiden, The Netherlands

J. V. Sengers (✉)  
Institute for Physical Science and Technology, University of Maryland, College Park,  
MD 20742, USA  
e-mail: sengers@umd.edu

J. V. Sengers  
Department of Mechanical Engineering, University of Maryland, College Park,  
MD 20742, USA

the locus of vapor–liquid critical points, also referred to as plait points, is more complex. Early theoretical predictions for the asymptotic critical behavior of the various transport properties of fluid mixtures have been proposed by Gorodetskii and coworkers [3,4] and by Mistura [5]. The theory for the behavior of the transport properties in binary mixtures near the vapor–liquid critical line was further pursued by Onuki with the special aim of interpreting experimental transport-property data for mixtures of  $^3\text{He}$  and  $^4\text{He}$  [6]. Mostert and Sengers [7] and Anisimov and coworkers [8,9] have considered the effects of noncritical contributions to the Onsager coefficients on the expected asymptotic behavior of the transport coefficients of fluid mixtures in the vicinity of critical points. Theoretical expressions, which also include the nonasymptotic critical behavior of the transport properties of mixtures, have been developed by Luettmmer-Strathmann and Sengers [10] and by Kiselev and Kulikov [11]. An alternative theoretical description of the critical behavior of the transport properties of mixtures has been developed by Folk and Moser [12] on the basis of a dynamic renormalization group theory. All theories predict that the thermal conductivity of fluid mixtures should remain finite on the critical locus except at an azeotropic critical point.

Early measurements of the thermal conductivity of fluid mixtures near plait points have been reported by Cohen et al. [13,14] for mixtures of  $^3\text{He}$  and  $^4\text{He}$  and by Friend and Roder [15,16] for mixtures of methane and ethane. These measurements showed a pronounced critical enhancement of the thermal conductivity similar to that observed in one-component fluids, and any crossover to the predicted finite asymptotic behavior of the thermal conductivity was not observed even though in the case of mixtures of  $^3\text{He}$  and  $^4\text{He}$  the measurements included thermal-conductivity data very close to the plait point [17,18]. The first direct experimental confirmation that the thermal conductivity does not diverge at the critical point of mixtures but crosses over to a finite limiting behavior at the vapor–liquid critical point was obtained by Sakonidou et al. [19] for an equimolar mixture of methane and ethane.

In the present article we report experimental data obtained for the thermal conductivity of mixtures of carbon dioxide and ethane in the critical region. The  $\text{CO}_2 + \text{C}_2\text{H}_6$  system exhibits critical azeotropy [20] and, hence, we expect the critical behavior of mixtures of carbon dioxide and ethane to be different from that observed for mixtures of methane and ethane. The thermal conductivity of the individual components, carbon dioxide and ethane, in the critical region has been measured previously by us [21,22].

## 2 Experimental Method

The thermal conductivity of mixtures of carbon dioxide and ethane was measured with the same parallel-plate apparatus that was used for the determination of the thermal conductivity of ethane in the critical region [22]. Since this apparatus has been described in detail in an earlier publication [23], a brief discussion of the experimental method will suffice. As in all parallel-plate instruments, heat is generated in an upper plate and transported through a horizontal fluid layer to a lower plate. The upper plate is surrounded by a guard ring to ensure that heat is transferred through the fluid layer

only. The guard ring is kept at the same temperature as the upper plate throughout the measurement. The fluid surrounds the cell and fills the gaps between the plates.

In our instrument, all sections of the upper plate, lower plate, and guard ring are made of electrolytic copper. Heater and thermometer wires are made of platinum and are located in grooves which are fraised in sections of the plates. The wires are electrically insulated from the copper plates by means of beryllium oxide beads. The height  $d$  of the gap between the upper and lower plates is fixed by three circular glass spacers. The guard plate is surrounded by a cap made of kufalit. The thermal expansion coefficient of this material is comparable to that of copper.

The thermal conductivity coefficient  $\lambda$  is calculated to first order from the relation

$$\lambda = \frac{Qd}{A\Delta T}. \quad (1)$$

Here,  $Q$  is the heat transferred from the upper plate to the lower plate by conduction,  $A$  is the effective area of the upper plate, and  $\Delta T$  is the temperature difference between the upper and lower plates. Some corrections have to be applied to Eq. 1, which are at most of the order of a few percent [23].

Especially near a critical point, a major source of error in thermal-conductivity measurements can be heat transported by convection [24]. In order to reduce the possibility of convection, a small gap distance was used ( $d = (147 \pm 2) \mu\text{m}$ ), while the temperature difference was varied from values as large as 100 mK far from the critical point to values as small as (1–2) mK very close to the critical point. The absence of convective heat transfer was checked by measuring with different values of the temperature difference  $\Delta T$  between the upper and lower plates.

The thermal-conductivity cell is located inside a high-pressure vessel that is surrounded by a cryostat which is suitable for temperatures down to the boiling temperature of liquid nitrogen. For the experiments reported here, the high-pressure vessel was surrounded by air for measurements above room temperature and by nitrogen vapor boiled off liquid nitrogen for measurements below room temperature. The temperature of the thermostat was controlled to within  $\pm 1$  mK. The actual average temperature at which the thermal conductivity was obtained has a possible uncertainty of  $\pm 0.01$  K. The pressure of the fluid was transferred to oil via a mercury-piston gas compressor and measured with a dead-weight gauge. The pressures have been determined with an uncertainty of  $\pm 0.005$  MPa. Further information about the thermal-conductivity apparatus and the measurement procedure can be found elsewhere [23, 25].

The auxiliary system for filling the pressure vessel with the gas mixture could be heated electrically to a temperature above 315 K, which is well above the critical temperature of the  $\text{CO}_2 + \text{C}_2\text{H}_6$  mixtures at any concentration. In this way demixing of the gases in the filling system was avoided. The experiments were performed with four different mixtures with mole fractions  $x$  of  $\text{CO}_2$  corresponding to  $x = 0.2500$ ,  $x = 0.2604$ ,  $x = 0.5000$ , and  $x = 0.7398$ . The mixture exhibits critical azeotropy at  $x \simeq 0.72$  [20, 26]. The mixtures were prepared gravimetrically by Matheson from ethane with a stated purity of 99.99 % and carbon dioxide with a stated purity of 99.998 % and were supplied in  $0.050 \text{ m}^3$  cylinders. The composition of the mixtures prior to the experiments was guaranteed with an uncertainty of  $\pm 0.02$  %.

**Table 1** Critical parameters of  $x\text{CO}_2 + (1-x)\text{C}_2\text{H}_6$  from Ref. [28]

$x$	$T_c$ (K)	$\rho_c$ (mol · L <sup>-1</sup> )	$p_c$ (MPa)
0.2500	296.239	7.536	5.29
0.2604	295.939	7.567	5.31
0.5000	291.111	8.346	5.68
0.7398	292.936	9.305	6.24

The experimental information for the critical temperature  $T_c$ , the critical density  $\rho_c$ , and the critical pressure  $p_c$  of mixtures of carbon dioxide and ethane has been reviewed by Abbaci et al. [27] and, more recently, by Sengers and Jin [28]. The values for the critical parameters of the mixtures as calculated from the equations recommended by Sengers and Jin are presented in Table 1.

### 3 Experimental Results

For each mixture the thermal conductivity was measured as a function of the temperature  $T$  at constant density  $\rho$ . Measurements at near-critical isochores were performed for all four mixtures. The measurements for the  $x = 0.2500$  mixture are the most extensive and span a reduced density range from  $\rho/\rho_c = 0.063$  to  $\rho/\rho_c = 1.482$ . The temperature range extends from 318 K, which corresponds to  $(T - T_c)/T_c \simeq 0.1$ , to slightly below the critical temperature. With the electronic system, it was usually possible to do two, and occasionally three, partially automated measurements with different temperature differences  $\Delta T$  on a single day.

To determine the density of each isochore, the pressure  $p$  was measured at a temperature of about 318 K, which is about 22 K above the critical temperature of the  $x = 0.2500$  and  $x = 0.2604$  mixtures and about 25 K above the critical temperature of the  $x = 0.5000$  and  $x = 0.7398$  mixtures. At this temperature the density was calculated from the observed pressure and temperature with the aid of an equation of state. For this purpose, we have used a fundamental equation for the Helmholtz free-energy density developed by Jin [29]. This equation, which is an improved version of an earlier fundamental equation [30], satisfies the theoretically predicted scaling laws for binary fluid mixtures and incorporates crossover to analytic behavior far from the critical point. At the lowest density of the mixtures, the density is outside the range of validity of the equation for the critical region, and here we used an analytic equation of state, called DDMIX, developed by Ely and coworkers at the National Institute of Standards and Technology [31, 32]. The values, thus obtained for the isochoric densities, together with the corresponding temperatures and pressures, are presented in Table 2.

The experimental values obtained for the thermal conductivity of the four mixtures are presented in Tables 3–6. The first column in these tables gives the isochoric density  $\rho$ , the second column gives the temperature  $T$ , the third column gives the measured thermal conductivity  $\lambda$  at this temperature, and the last column gives the smallest temperature difference  $\Delta T$  employed in the measurements.

**Table 2** Isochoric densities of  $x\text{CO}_2 + (1-x)\text{C}_2\text{H}_6$ 

$x$	$T$ (K)	$p$ (MPa)	$\rho$ (mol · L <sup>-1</sup> )
0.2500	318.133	1.109	0.446
0.2500	318.157	5.204	2.94
0.2500	318.264	7.098	5.68
0.2500	318.131	7.593	6.83
0.2500	318.139	7.608	6.87
0.2500	318.136	7.860	7.45
0.2500	318.126	7.878	7.49
0.2500	318.230	8.371	8.45
0.2500	318.130	10.523	10.78
0.2604	318.066	1.970	0.877
0.2604	318.393	5.277	3.09
0.2604	318.172	7.587	6.71
0.5000	318.126	1.091	0.435
0.5000	318.122	5.483	2.94
0.5000	318.127	7.831	5.65
0.5000	318.107	8.563	6.96
0.5000	318.139	8.864	7.53
0.5000	318.098	8.965	7.73
0.7398	318.125	8.711	6.63
0.7398	318.037	9.939	9.12

The estimated accuracy of the experimental thermal-conductivity data is the same as the accuracy of the thermal-conductivity data for ethane [22] at the same reduced temperatures and densities. Hence, also for the mixtures the uncertainty of the thermal-conductivity not close to the critical point is of the order of 1 % and increases to about 5 % near the critical point. The increase of the experimental uncertainty in the near vicinity of the critical point has several origins. First, the uncertainty in  $\lambda$  increases, because of the necessary use of very small values of  $\Delta T$ . Second, the assumption that the density  $\rho$  at which the thermal conductivity is measured equals the density determined at the reference temperature of 318 K is only approximately valid. In principle, near the critical point the density should be corrected for a gravitationally induced density gradient and a temperature-gradient induced density gradient, as in the case of a one-component fluid [22,23]. Also, gravitationally induced concentration gradients and temperature-gradient induced concentration gradients may be considered. The effect on the density is roughly of the same magnitude as in the case of one-component fluids [22], which gives very close to the critical point an uncertainty in the density of about  $\pm 0.1 \text{ mol} \cdot \text{L}^{-1}$ . The gravitationally induced concentration gradients for our mixture, which exhibits critical azeotropy, are very small. Model calculations of Chang et al. [33] have shown that at the critical isochore of the equimolar mixture the predicted concentration difference is still only 0.001 at  $T - T_c = 2 \text{ mK}$ .

The experimental data in Tables 3–5 are close to, but not completely identical to, the values in the original thesis dealing with this research [25]. First of all, the temperatures have been converted from IPTS-68 to ITS-90. Second, the isochoric densities were calculated from an improved equation of state for  $\text{CO}_2 + \text{C}_2\text{H}_6$  in the critical region [29]. Finally, subsequent recalibration of some of the instrumental constants led to a lowering of the original thermal-conductivity values by about 2 % (H.R. van den Berg and E.P. Sakonidou, 1993, private communication).

**Table 3** Thermal conductivity of  $x\text{CO}_2 + (1-x)\text{C}_2\text{H}_6$  at  $x = 0.25$  ( $\Delta T$  represents the smallest temperature difference employed in the measurements)

$\rho$ (mol · L <sup>-1</sup> )	$T$ (K)	$\lambda$ (mW · m <sup>-1</sup> · K <sup>-1</sup> )	$\Delta T$ (mK)
0.446	318.152	23.2	22.4
0.446	308.075	21.9	20.8
0.446	302.023	21.4	22.1
0.446	299.020	21.2	40.6
0.446	299.010	21.1	41.3
0.446	297.517	21.0	41.8
0.446	296.880	21.0	40.7
0.446	296.565	20.9	40.2
0.446	296.125	20.9	41.0
2.94	318.164	31.6	11.5
2.94	308.149	31.0	20.9
2.94	302.041	30.7	20.5
2.94	298.996	30.5	4.89
2.94	297.470	30.5	11.1
2.94	296.864	30.6	20.0
2.94	296.516	30.8	20.3
2.94	296.242	31.2	5.34
2.94	296.141	30.4	3.59
5.68	318.272	48.1	10.3
5.68	308.701	51.6	9.05
5.68	302.017	56.0	4.54
5.68	298.992	62.3	3.97
5.68	297.459	67.7	9.04
5.68	296.847	72.9	3.96
5.68	296.451	71.9	3.95
5.68	296.293	75.7	4.35
5.68	296.188	75.1	4.08
5.68	296.183	75.0	5.14
6.83	318.139	53.2	5.09
6.83	308.011	56.7	4.80
6.83	302.035	65.8	9.25
6.83	301.995	65.8	4.61
6.83	298.988	77.9	4.64
6.83	297.467	102	8.60
6.83	297.465	102	2.19
6.83	297.456	110	4.46
6.83	296.842	142	1.53
6.83	296.791	218	3.25
6.83	296.741	199	1.68
6.83	296.656	138	2.00
6.83	296.461	102	1.97
6.83	296.221	85.5	6.76
6.83	296.197	90.9	4.30
6.87	296.826	157	2.20
6.87	296.800	168	1.94
6.87	296.766	195	1.69
6.87	296.764	189	1.84
6.87	296.748	204	1.62
6.87	296.733	195	1.64
6.87	296.711	214	3.53
6.87	296.703	188	3.40
6.87	296.701	177	1.91
6.87	298.685	169	3.77

**Table 3** continued

$\rho$ (mol · L <sup>-1</sup> )	$T$ (K)	$\lambda$ (mW · m <sup>-1</sup> · K <sup>-1</sup> )	$\Delta T$ (mK)
7.45	308.060	64.6	2.24
7.45	298.954	81.0	2.25
7.45	296.881	145	1.85
7.45	296.755	157	1.95
7.45	296.737	145	2.48
7.45	296.721	166	2.00
7.45	296.716	164	1.48
7.45	296.708	175	3.51
7.45	296.699	154	2.30
7.45	296.687	186	1.67
7.45	296.646	183	1.66
7.45	296.640	186	1.55
7.45	296.620	184	1.57
7.45	296.579	157	1.91
7.45	296.524	131	2.12
7.45	296.406	117	2.18
7.45	296.402	124	1.84
7.45	296.222	99.0	2.07
7.45	296.218	88.8	2.08
7.45	296.072	88.8	2.26
7.45	295.975	88.1	3.78
7.45	295.871	83.3	2.71
7.45	295.756	84.3	4.10
7.45	295.606	79.5	3.65
7.49	318.135	55.9	5.46
7.49	308.020	61.4	5.61
7.49	302.060	69.9	4.54
7.49	298.989	81.1	4.05
7.49	297.481	111	3.79
7.49	296.880	139	3.64
7.49	296.541	166	8.64
7.49	296.442	130	2.13
7.49	296.441	124	4.16
7.49	296.397	114	2.08
7.49	296.337	107	4.16
7.49	296.306	102	2.26
7.49	296.183	91.4	4.06
8.45	318.164	49.0	2.74
8.45	308.226	61.7	4.48
8.45	302.049	67.6	9.16
8.45	297.443	82.1	4.27
8.45	296.802	92.1	2.38
8.45	296.215	107	2.45
8.45	296.106	110	2.20
8.45	296.057	112	2.12
10.78	318.145	65.0	9.20
10.78	308.116	65.9	9.88
10.78	298.988	68.4	8.50
10.78	297.499	67.1	4.81
10.78	296.143	69.2	3.82

**Table 4** Thermal conductivity of  $x\text{CO}_2 + (1-x)\text{C}_2\text{H}_6$  at  $x = 0.26$  ( $\Delta T$  represents the smallest temperature difference employed in the measurements)

$\rho$ (mol · L <sup>-1</sup> )	$T$ (K)	$\lambda$ (mW · m <sup>-1</sup> · K <sup>-1</sup> )	$\Delta T$ (mK)
0.877	318.193	23.6	78.7
0.877	308.095	22.8	75.1
0.877	302.009	22.2	36.4
0.877	296.870	21.7	70.2
0.877	293.153	21.3	35.6
3.09	318.165	31.8	40.7
3.09	308.158	31.4	18.7
3.09	302.105	31.1	38.1
3.09	297.156	31.3	37.6
3.09	293.641	31.4	17.4
6.71	318.207	50.3	10.0
6.71	308.182	54.0	19.1
6.71	301.934	62.4	9.10
6.71	296.866	110	4.28
6.71	296.844	111	3.61
6.71	296.816	118	8.60
6.71	296.516	135	9.20
6.71	296.435	167	4.24
6.71	296.396	180	3.70
6.71	296.394	166	8.26
6.71	296.381	193	3.57
6.71	296.381	172	3.40
6.71	296.375	147	4.12
6.71	296.362	166	8.04
6.71	296.343	159	3.83
6.71	296.236	118	8.45
6.71	296.096	95.8	4.27
6.71	296.054	101	7.25
6.71	296.053	99.0	4.53
6.71	295.732	84.5	9.02
6.71	294.960	75.0	4.15
6.71	293.082	68.7	4.73

The thermal-conductivity measurements for a number of the isochores for the  $x = 0.25$  mixtures are shown as a function of temperature in Figs. 1 and 2. As can be seen from Fig. 1, at the lowest and highest densities the thermal conductivity varies only slowly with temperature and any critical enhancement is small. However, as shown in Fig. 2, at densities near the critical density, the thermal conductivity increases rapidly when the temperature approaches the critical temperature. The same phenomenon is observed for the near-critical isochores of the other mixtures as shown in Figs. 3–5. As to be discussed in the next section, we expect the thermal conductivity to diverge at the critical point for mixtures with a concentration near  $x = 0.72$  corresponding to the critical azeotropic concentration, but the thermal conductivity is expected to go to a finite limiting value at the critical point for mixtures with a concentration that differs from the azeotropic concentration. Originally we appeared to observe that the thermal conductivity of the  $x = 0.25$  and  $x = 0.50$  mixtures tended to increase rapidly upon approach to the critical temperature, but then after going through a finite maximum in the one-phase region would decrease very close to the critical temperature; we interpreted this observation as evidence for a finite thermal-conductivity



**Table 5** Thermal conductivity of  $x\text{CO}_2 + (1-x)\text{C}_2\text{H}_6$  at  $x = 0.50$  ( $\Delta T$  represents the smallest temperature difference employed in the measurements)

$\rho$ (mol · L <sup>-1</sup> )	$T$ (K)	$\lambda$ (mW · m <sup>-1</sup> · K <sup>-1</sup> )	$\Delta T$ (mK)
0.435	318.110	21.8	23.0
0.435	308.087	20.7	20.7
0.435	308.074	20.7	21.5
0.435	301.977	20.3	20.1
0.435	296.055	19.6	20.5
0.435	293.155	19.3	20.8
0.435	292.083	19.2	19.5
0.435	291.505	19.2	20.0
0.435	291.336	19.2	39.8
0.435	291.085	19.1	40.6
2.94	318.143	29.3	20.9
2.94	307.987	27.9	9.90
2.94	302.010	28.1	20.9
2.94	296.073	27.8	19.4
2.94	293.130	27.7	19.6
2.94	292.109	27.6	20.5
2.94	291.547	27.4	8.60
2.94	291.340	27.4	9.10
2.94	291.055	27.6	9.27
5.65	318.149	39.8	4.04
5.65	318.132	41.1	10.0
5.65	308.062	41.0	9.79
5.65	302.433	43.6	5.45
5.65	296.035	47.0	11.3
5.65	293.144	52.0	4.69
5.65	292.093	54.6	9.49
5.65	291.569	55.3	4.54
5.65	291.350	54.2	4.30
5.65	291.072	55.4	4.16
6.96	318.128	42.5	9.82
6.96	308.016	46.8	4.85
6.96	301.958	53.1	4.65
6.96	296.073	62.0	4.41
6.96	295.697	63.9	4.62
6.96	293.086	86.1	2.18
6.96	292.054	99.0	4.24
6.96	292.054	91.3	2.20
6.96	291.347	111	4.28
6.96	291.341	110	2.02
6.96	291.178	108	2.01
6.96	291.172	110	1.99
6.96	291.112	104	2.12
6.96	291.058	99.0	1.95
7.53	318.115	44.5	4.04
7.53	308.029	46.9	4.89
7.53	301.946	50.5	2.38
7.53	296.022	64.2	4.17
7.53	293.083	83.3	4.21
7.53	292.052	106	1.78
7.53	291.567	139	3.88
7.53	291.347	172	1.59
7.53	291.333	206	0.67

**Table 5** continued

$\rho$ (mol · L <sup>-1</sup> )	$T$ (K)	$\lambda$ (mW · m <sup>-1</sup> · K <sup>-1</sup> )	$\Delta T$ (mK)
7.53	291.318	210	1.48
7.53	291.294	158	1.87
7.53	291.257	159	1.70
7.53	291.200	144	1.60
7.53	291.067	114	2.41
7.73	318.131	40.3	5.41
7.73	308.005	46.2	6.10
7.73	301.907	49.3	2.56
7.73	296.021	59.5	4.67
7.73	293.111	79.8	2.39
7.73	292.051	102	2.24
7.73	291.551	128	1.46
7.73	291.336	203	1.43
7.73	291.236	151	2.02

**Table 6** Thermal conductivity of  $x\text{CO}_2 + (1-x)\text{C}_2\text{H}_6$  at  $x = 0.74$  ( $\Delta T$  represents the smallest temperature difference employed in the measurements)

$\rho$ (mol · L <sup>-1</sup> )	$T$ (K)	$\lambda$ (mW · m <sup>-1</sup> · K <sup>-1</sup> )	$\Delta T$ (mK)
6.63	318.111	38.2	10.4
6.63	308.179	41.3	21.2
6.63	302.253	43.6	9.67
6.63	299.010	46.7	9.41
6.63	296.055	50.6	9.56
6.63	296.050	50.7	4.77
6.63	293.153	57.8	9.86
6.63	292.638	59.3	5.06
9.12	318.038	35.4	11.0
9.12	308.064	48.5	9.56
9.12	298.485	60.0	4.72
9.12	296.032	66.3	2.76
9.12	294.723	82.4	2.52
9.12	294.325	84.2	1.59
9.12	293.952	101	5.23
9.12	293.531	116	2.30
9.12	293.339	135	2.34
9.12	293.239	156	2.49
9.12	293.168	160	1.44
9.12	293.154	213	2.52

value near criticality for these mixtures [7,25]. However, it was realized subsequently that this phenomenon could be attributed to a small change of the actual composition of the mixture in the layer between the two plates caused by preferential absorption of the carbon dioxide into the kufalit insulation gap. A quantitative analysis of this absorption effect was made by Sakonidou et al. [19], who showed that it could readily account for an increase of the critical temperature in the layer between the plates by an amount comparable to the small temperature range in which a decrease of the thermal conductivity had been observed. We, thus, concluded that the two-phase region had been entered at a slightly higher temperature than the nominal critical temperature attributed to the mixture. The few data points that, in retrospect, correspond to temperatures below the transition temperatures have not been included in Figs. 1–5.

**Fig. 1** Thermal conductivity of a mixture of 25 mol% carbon dioxide and 75 mol% ethane along three off-critical isochores as a function of temperature. Symbols indicate the experimental data, and curves represent values calculated from the mode-coupling theory by Luettmer-Strathmann and Sengers [10]

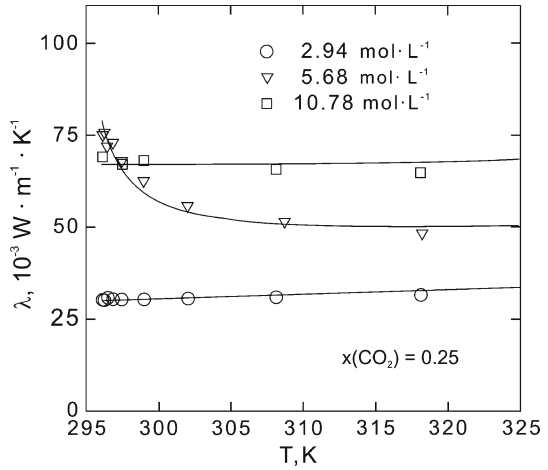


**Fig. 2** Thermal conductivity of a mixture of 25 mol% carbon dioxide and 75 mol% ethane along near-critical isochores as a function of temperature. Symbols indicate the experimental data and the curve represents values calculated from the mode-coupling theory by Luettmer-Strathmann and Sengers [10]

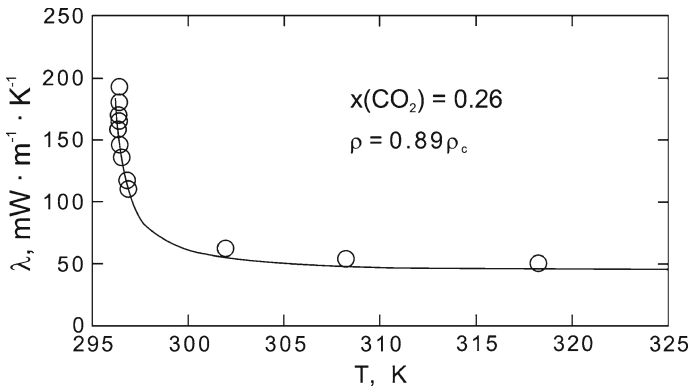
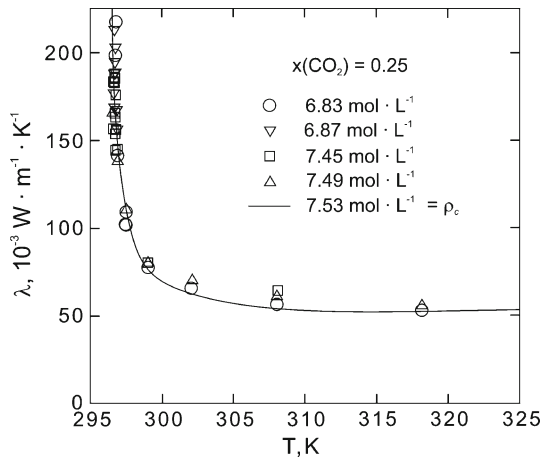


**Fig. 3** Thermal conductivity of a mixture of 26 mol% carbon dioxide and 74 mol% ethane along a near-critical isochore as a function of temperature. Symbols indicate the experimental data, and the solid curve represents the values calculated from the mode-coupling theory by Luettmer-Strathmann and Sengers [10]

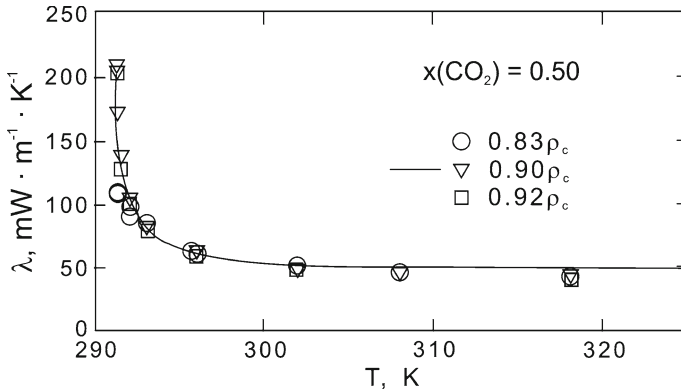


**Fig. 4** Thermal conductivity of a mixture of 50 mol% carbon dioxide and 50 mol% ethane along near-critical isochores as a function of temperature. Symbols indicate the experimental data, and the solid curve represents the values from the mode-coupling theory by Luettmer-Strathmann and Sengers [10]

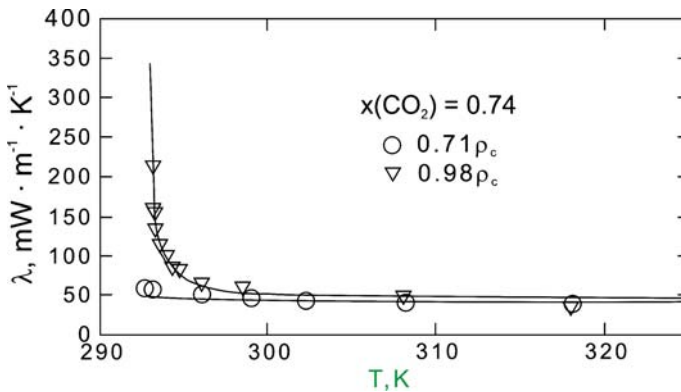


**Fig. 5** Thermal conductivity of a mixture of 74 mol% carbon dioxide and 26 mol% ethane along two isochores as a function of temperature. Symbols indicate the experimental data, and solid curves represent values calculated from the mode-coupling theory by Luettmer-Strathmann and Sengers [10]

#### 4 Comparison with Theory

For a theoretical interpretation of the critical behavior of transport properties, one needs to decompose all kinetic coefficients into a critical enhancement and a non-critical background contribution [2]. Specifically, for the thermal conductivity of a one-component fluid, this decomposition leads to an expression of the form [2]

$$\lambda = \Delta\lambda + \lambda_b. \quad (2)$$

Mode-coupling theory predicts that asymptotically close to the critical point the critical thermal-conductivity enhancement  $\Delta\lambda$  satisfies a Stokes-Einstein relation of the form

$$\Delta\lambda = \frac{R_D k_B T \rho}{6\pi \eta \xi} c_p, \tag{3}$$

where  $R_D \simeq 1.05$  is a universal dynamic amplitude ratio [34,35],  $k_B$  is Boltzmann’s constant,  $\eta$  is the shear viscosity,  $\xi$  is the correlation length, and  $c_p$  is the isobaric specific heat capacity. In a one-component fluid  $c_p$  diverges much faster than the product  $\eta\xi$  and the thermal conductivity diverges at the critical point [22].

For a binary fluid one starts from the linear relations relating the diffusion current  $\mathbf{J}_d$  and the heat current  $\mathbf{J}_q$  to the chemical-potential gradient  $\nabla\mu$  and the temperature gradient  $\nabla T$ :

$$\mathbf{J}_d = -\alpha\nabla\mu - \beta\nabla T, \tag{4}$$

$$\mathbf{J}_q = -\delta\nabla\mu - \gamma\nabla T + \mu\mathbf{J}_d, \tag{5}$$

where  $\alpha, \beta, \gamma,$  and  $\delta$  are Onsager kinetic coefficients and where  $\mu$  is the chemical-potential difference between the two components [36]. Note that, because of the Onsager reciprocal relations,  $\delta = T\beta$ . The thermal conductivity  $\lambda$  of the mixture is defined by

$$\mathbf{J}_q = -\lambda\nabla T, \quad \mathbf{J}_d = 0, \tag{6}$$

such that the thermal conductivity is related to the Onsager kinetic coefficients by

$$\lambda = (\alpha\gamma - \beta\delta) / \alpha. \tag{7}$$

The kinetic coefficients are to be separated into a critical part and a noncritical part similarly to the decomposition of the thermal conductivity coefficient of a one-component fluid, given by Eq. 2 [7–11]:

$$\alpha = \Delta\alpha + \alpha_b, \beta = \Delta\beta + \beta_b, \gamma = \Delta\gamma + \gamma_b. \tag{8}$$

It follows from the mode-coupling theory that  $\Delta\alpha, \Delta\beta,$  and  $\Delta\gamma$  satisfy Stokes-Einstein relations similar to the one given by Eq. 3 [5]:

$$\Delta\alpha = \frac{k_B T \rho}{6\pi \eta \xi} \left( \frac{\partial x}{\partial \mu} \right)_{T,p}, \tag{9}$$

$$\Delta\beta = \frac{k_B T \rho}{6\pi \eta \xi} \left( \frac{\partial x}{\partial T} \right)_{\mu,p}, \tag{10}$$

$$\Delta\gamma = \frac{k_B T \rho}{6\pi \eta \xi} c_{p,\mu}, \tag{11}$$

where  $c_{p,\mu}$  is the isobaric specific heat capacity at constant field  $\mu$  and where we have approximated the constant  $R_D$  in Eq. 3 by unity. Substituting the equations for the kinetic coefficients into Eq. 7 and using some thermodynamic relations, one obtains for the thermal conductivity [7],

$$\lambda = \frac{k_B T \rho}{6\pi \eta \xi} \left( \frac{\Delta\alpha}{\alpha} c_{p,x} + \frac{\alpha_b}{\alpha} c_{p,\mu} \right) - \frac{T\beta_b}{\alpha} (2\Delta\beta + \beta_b) + \gamma_b. \quad (12)$$

We note that the asymptotic expressions in Eqs. 9 and 10 are not independent, but related by  $\Delta\beta = -(\partial\mu/\partial T)_{p,x} \Delta\alpha$  [10]. For the interpretation of Eq. 12, one can distinguish between two regimes. Away from the critical point ( $\Delta\alpha \ll \alpha_b$ ,  $\Delta\beta \ll \beta_b$ ), the expression for the thermal conductivity reduces to

$$\lambda = \frac{k_B T \rho}{6\pi \eta \xi} c_{p,\mu} - \frac{T\beta_b^2}{\alpha} + \gamma_b. \quad (13)$$

The first term on the right-hand side (RHS) of Eq. 13 diverges like the thermal conductivity of a one-component fluid, because  $c_{p,\mu}$  of a mixture diverges like  $c_p$  of a one-component fluid [37]. Very close to the critical point ( $\Delta\alpha \gg \alpha_b$ ,  $\Delta\beta \gg \beta_b$ ), one obtains

$$\lambda = \frac{k_B T \rho}{6\pi \eta \xi} c_{p,x} + \frac{1}{\alpha} \left( \frac{k_B T \rho}{6\pi \eta \xi} \alpha_b c_{p,\mu} - 2T\beta_b \Delta\beta \right) + \gamma_b. \quad (14)$$

The first term on the RHS of Eq. 14 vanishes as the critical point is approached, since the isobaric specific heat capacity at constant pressure and concentration diverges only weakly at the critical point [36]. An exception is an azeotropic critical mixture in which  $c_{p,x}$  continues to diverge like  $c_p$  of a one-component fluid [38]. The third term represents a background contribution like in a one-component fluid. The second term goes asymptotically near the critical point to a finite value.

Equations 9–11 represent predictions of the mode-coupling theory for the asymptotic critical behavior of the critical enhancements of the kinetic coefficients. Just as for a quantitative interpretation of the thermal-conductivity data of one-component fluids in the critical region [22, 34], one needs to extend the mode-coupling theory to include non-asymptotic critical contributions to the enhancements as well as a crossover to non-critical behavior of the transport properties far away from the critical point, where the kinetic coefficients should approach their background values. An analysis of our experimental data in terms of such a more general mode-coupling theory, which asymptotically near the critical point reduces to Eq. 12 for the thermal conductivity, has been made by Luettmmer-Strathmann and Sengers [10] and also by Kiselev and Huber [39]. There is no reason to repeat the analysis here. Instead, we simply show in Figs. 1–5 the values calculated for the thermal conductivity by Luettmmer-Strathmann and Sengers [10] with system-dependent background contributions appropriate for  $\text{CO}_2 + \text{C}_2\text{H}_6$ . We conclude that the observed temperature dependence of the thermal conductivity is well described by the mode-coupling theory of critical dynamics in mixtures. In

**Fig. 6** Temperature dependence of the critical enhancement  $\Delta\lambda$  along the critical isochores of three mixtures of carbon dioxide and ethane calculated from the mode-coupling theory; mixtures of carbon dioxide and ethane exhibit critical azeotropy at  $x(\text{CO}_2) \simeq 0.72$ ; from Ref. [10]

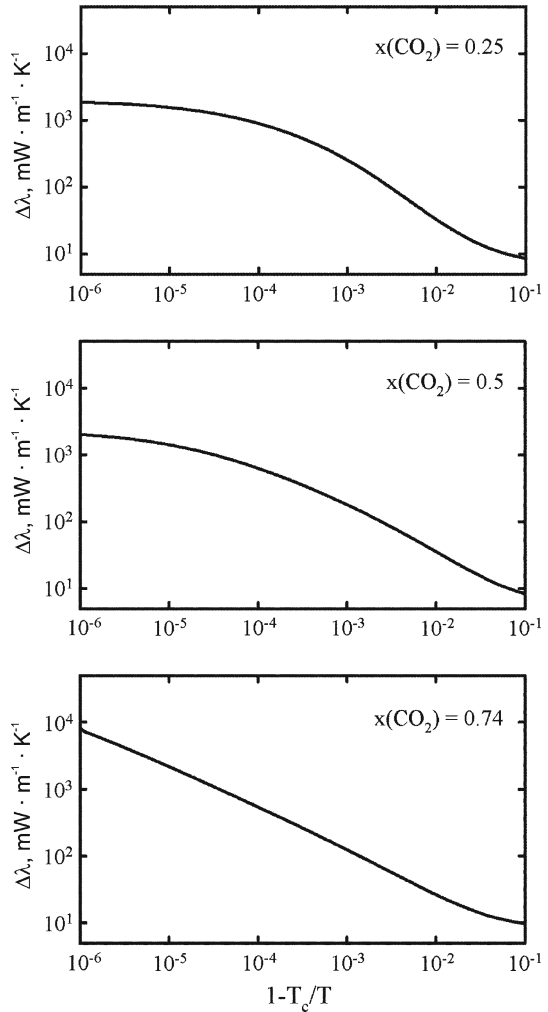


Fig. 6 we show the thermal conductivity calculated from the same mode-coupling theory as a function of  $1 - T/T_c$  for the  $x = 0.25$ ,  $x = 0.50$ , and  $x = 0.74$  mixtures. It is seen that at  $x = 0.74$  the thermal conductivity continues to diverge, but at  $x = 0.25$  and  $x = 0.50$ , the thermal conductivity indeed crosses over to a finite limit, as indeed predicted by the asymptotic theory. However, this crossover behavior to a finite limit occurs at temperatures a bit closer to the critical temperature than those readily accessible with our instrument.

## 5 Conclusion

We have measured the thermal conductivity of four mixtures of carbon dioxide and ethane in the critical region as a function of density and temperature. The experimental

data agree with the behavior of the thermal conductivity calculated from the mode-coupling theory of critical dynamics for the mixtures and are consistent with the theoretical prediction of a divergent thermal conductivity at the azeotropic critical temperature and a crossover to a finite limiting value at nonazeotropic critical temperatures.

**Acknowledgments** We dedicate this article to the memory of Hans R. van den Berg who was our collaborator in this research. We also acknowledge assistance of Peter S. van der Gulik in the initial stage of the project. The experiments were performed in the Van der Waals-Zeeman Institute at the University of Amsterdam. The authors are indebted to Jutta Luettmer-Strathmann for a theoretical analysis of our experimental data.

## References

1. J.V. Sengers, P.H. Keyes, Phys. Rev. Lett. **62**, 70 (1971)
2. J.V. Sengers, Int. J. Thermophys. **6**, 203 (1985)
3. M.Sh. Gitterman, E.E. Gorodetskii, Sov. Phys. JETP **30**, 348 (1970)
4. M.A. Anisimov, A.V. Voronel, E.E. Gorodetskii, Sov. Phys. JETP **33**, 605 (1972)
5. L. Mistura, Nuovo Cimento **12B**, 35 (1972); J. Chem. Phys. **62**, 4571 (1975)
6. A. Onuki, J. Low Temp. Phys. **61**, 101 (1985)
7. R. Mostert, J.V. Sengers, Fluid Phase Equilib. **75**, 235 (1992); **85**, 347 (1993)
8. M.A. Anisimov, S.B. Kiselev, Int. J. Thermophys. **13**, 873 (1992)
9. M.A. Anisimov, E.E. Gorodetskii, V.D. Kulikov, A.A. Povodyrev, J.V. Sengers, Physica A **220**, 277 (1995); **223**, 272 (1996)
10. J. Luettmer-Strathmann, J.V. Sengers, J. Chem. Phys. **104**, 3026 (1996); **106**, 438 (1997)
11. S.B. Kiselev, V.D. Kulikov, Int. J. Thermophys. **15**, 283 (1994); **18**, 1143 (1997)
12. R. Folk, G. Moser, J. Low Temp. Phys. **99**, 11 (1995); Condensed Matter Phys. **7**, 27 (1996); Phys. Rev. E **58**, 6246 (1998)
13. L.H. Cohen, M.L. Dingus, H. Meyer, J. Low Temp. Phys. **49**, 545 (1982); **61**, 79 (1985)
14. L.H. Cohen, M.L. Dingus, H. Meyer, Phys. Rev. Lett. **50**, 1058 (1983)
15. D.G. Friend, H.M. Roder, Phys. Rev. A **32**, 1941 (1985)
16. H.M. Roder, D.G. Friend, Int. J. Thermophys. **6**, 607 (1985)
17. H. Meyer, L.H. Cohen, Phys. Rev. A **38**, 2081 (1988)
18. R. Folk and G. Moser, Int. J. Thermophys. **16**, 1363 (1995)
19. E.P. Sakonidou, H.R. van den Berg, C.A. ten Seldam, J.V. Sengers, J. Chem. Phys. **109**, 717 (1998)
20. J.C. Rainwater, in *Supercritical Fluid Technology: Reviews in Modern Theory and Applications*, ed. by T.J. Bruno, J.F. Ely (CRC Press, Boca Raton, Florida, 1991), p. 57
21. A. Michels, J.V. Sengers, P.S. van der Gulik, Physica **28**, 1216 (1962).
22. R. Mostert, P.S. van der Gulik, J.V. Sengers, J. Chem. Phys. **92**, 5454 (1990).
23. R. Mostert, H.R. van den Berg, P.S. van der Gulik, Rev. Sci. Instrum. **60**, 3466 (1989)
24. A. Michels, J.V. Sengers, Physica **28**, 1238 (1962).
25. R. Mostert, *The Thermal Conductivity of Ethane and of its Mixtures with Carbon Dioxide in the Critical Region* (Ph.D. Thesis, Van der Waals-Zeeman Institute, University of Amsterdam, Amsterdam, 1991)
26. A. Fredenslund, J. Mollerup, J. Chem. Soc. Faraday Trans. I **70**, 1653 (1974)
27. A. Abbaci, H.R. van den Berg, E. Sakonidou, J.V. Sengers, Int. J. Thermophys. **13**, 1043 (1992)
28. J.V. Sengers, G.X. Jin, Int. J. Thermophys. **28**, 1181 (2007)
29. G.X. Jin, *Effects of Critical Fluctuations on the Thermodynamic Properties of Fluids and Fluid Mixtures* (Ph.D. Thesis, Institute for Physical Science and Technology, University of Maryland, College Park, Maryland, 1993)
30. G.X. Jin, S. Tang, J.V. Sengers, Phys. Rev. E **47**, 388 (1993)
31. G.J. Sherman, J.W. Magee, J.F. Ely, Int. J. Thermophys. **10**, 47 (1989)
32. J.F. Ely, J.W. Magee, in *Proceedings of the GPA 68th Annual Convention* (Gas Processors Association, Tulsa, Oklahoma 1989), p. 89
33. R.F. Chang, J.M.H. Levelt Sengers, T. Doiron, J. Jones, J. Chem. Phys. **79**, 3058 (1983)
34. J. Luettmer-Strathmann, J.V. Sengers, G.A. Olchowy, J. Chem. Phys. **103**, 7482 (1995)



35. S.K. Das, J. Horbach, K. Binder, M.E. Fisher, J.V. Sengers, *J. Chem. Phys.* **125**, 024506 (2006)
36. S.R. de Groot, P. Mazur, *Non-Equilibrium Thermodynamics* (Dover, New York, 1984)
37. R.B. Griffiths, J.C. Wheeler, *Phys. Rev. A* **2**, 1047 (1970)
38. M.A. Anisimov, E.E. Gorodetskii, V.D. Kulikov, J.V. Sengers, *Phys. Rev. E* **51**, 1199 (1995)
39. S.B. Kiselev, M.L. Huber, *Fluid Phase Equilib.* **142**, 253 (1998)